Published in final edited form as:
J Immunol. 2010 April 15; 184(8): 4557–4567. doi:10.4049/jimmunol.0902336.

Cell-Specific Gene Expression in Langerhans Cell Histiocytosis Lesions Reveals a Distinct Profile Compared to Epidermal Langerhans Cells1

Carl E. Allen[*,†], **Liunan Li**[*], **Tricia L. Peters**[‡], **Hon-chiu Eastwood Leung**[*,†,§], **Alexander Yu**[*], **Tsz-Kwong Man**[*,†], **Sivashankarappa Gurusiddappa**[*], **Michelle T. Phillips**[*], **M. John Hicks**[‡], **Amos Gaikwad**[*], **Miriam Merad**[¶], and **Kenneth L. McClain**[*,†]

[*]Texas Children's Cancer Center and Hematology Service, Department of Pediatrics, Baylor College of Medicine, Houston, TX 77030

[†]Dan L. Duncan Cancer Center, Baylor College of Medicine, Houston, TX 77030

[‡]Department of Pathology, Baylor College of Medicine, Houston, TX, 77030

[§]Department of Molecular and Cellular Biology, Baylor College of Medicine, Houston, TX 77030

[¶]Department of Gene and Cell Medicine, Mount Sinai School of Medicine, New York, NY 10029

Abstract

Langerhans-cell histiocytosis (LCH) is a rare disease characterized by heterogeneous lesions containing CD207+ Langerhans cells and lymphocytes that can arise in almost any tissue and cause significant morbidity and mortality. After decades of research, the cause of LCH remains speculative. A prevailing model suggests that LCH arises from malignant transformation and metastasis of epidermal Langerhans cells. In this study, CD207+ cells and CD3+ T cells were isolated from LCH lesions to determine cell-specific gene expression. Compared to control epidermal CD207+ cells, the LCH CD207+ cells yielded 2113 differentially-expressed genes (FDR<0.01). Surprisingly, expression of many genes previously associated with LCH, including cell-cycle regulators, pro-inflammatory cytokines and chemokines were not significantly different from control LCs in our study. However, several novel genes whose products activate and recruit T cells to sites of inflammation, including *SPP1* (osteopontin), were highly over-expressed in LCH CD207+ cells. Furthermore, several genes associated with immature myeloid dendritic cells were over-expressed in LCH CD207+ cells. Compared to the peripheral CD3+ cells from LCH patients, the LCH lesion CD3+ cells yielded only 162 differentially-regulated genes (FDR<0.01), and the expression profile of the LCH lesion CD3+ cells was consistent with an activated regulatory T cell phenotype with increased expression of *FOXP3*, *CTLA4* as well as *SPP1*. Results from this study support a model of LCH pathogenesis in which lesions do not arise from epidermal Langerhans cells, but from accumulation of bone-marrow derived immature myeloid dendritic cells that recruit activated lymphocytes.

[1]This study was supported in part by research funding from the Histiocytosis Association of America (CEA and KLM), the Histiocytosis Association of Canada (CEA and KLM), the American Society of Clinical Oncology (CEA), the Thrasher Research Fund (CEA), the Larry and Helen Hoag Foundation Clinical Translational Research Award (CEA), the US National Institutes of Health Pediatric Oncology Research Training Grant (T32 CA115303-03) (CEA) and (R21 CA 114981-01A2) (KLM). MTP received support from the American Cancer Society Institutional Research Grant (2007-08) #93-034-23.

Corresponding Author: Carl E. Allen MD, PhD, Texas Children's Hospital, 6621 Fannin St CC1410.00, Houston, TX 77030, (832)-824-4312 (Office), (832)-825-1453 (Fax), ceallen@txccc.org.

Keywords

Langerhans Cell Histiocyctosis; myeloid dendritic cells; gene expression

Introduction

Langerhans-cell histiocytosis (LCH) is a potentially fatal disease characterized by invasive lesions infiltrated with multiple cell types including CD1a+/CD207+ cells presumed to be pathologic Langerhans cells (LCs). The incidence of LCH is approximately 5 cases per million children and 1/10,000 live births per year (1). Approximately 30% as many adults are afflicted, though this incidence is likely underestimated (2). LCH includes a spectrum of clinical presentations from single system involvement in skin or bone, to diffuse multisystem involvement of liver, lungs, bone marrow, CNS and other organ systems (Reviewed in 3,4). Patients with limited organ system involvement have a very good prognosis, and patients with multisystem disease have survival rates of approximately 80% (5). However, survival is poor in patients with high risk multisystem disease who fail to respond to induction therapy (6). Chemotherapy for LCH is based on a lymphoma model of general immune suppression and cytotoxicity to rapidly proliferating cells (Reviewed in 7).

The etiology of LCH is not known. Scientific debate has focused on LCH resulting from malignant transformation or from functional proliferation of epidermal Langerhans cells in response to external stimuli (8–12). Regardless of whether or not clonal proliferation is the initiating factor in LCH, the CD207+ cells from these lesions require multiple interactions with other cell types including T cells, eosinophils and macrophages (13). LCs will not grow in isolation *in vitro* or as xenografts in immune-deficient mice. The mainstay of research on LCH tissues has been immunohistochemical analysis of biopsy samples. While this approach has been useful, it is also limited by various difficulties such as testing multiple antibodies simultaneously, variable sensitivity of antibodies, inability to quantitatively interpret results and lack of control tissues. RNA and protein studies from whole biopsy samples are also difficult to interpret due to the heterogeneous composition of LCH lesions. In order to overcome some of the experimental challenges in studying LCH, we have devised a robust procedure to study cell-specific gene expression profiling in the cells that most likely contribute to pathology in LCH patients: LCs (CD207+) and T cells (CD3+).

Materials and Methods

Subjects

LCH diagnosis was established by the presence of CD1a+ or CD207+ histiocytes in clinical biopsy specimens. Samples from the 15 individuals with LCH in this study included patients with relapsed disease and high risk multi-system disease (Supplemental Table IA). Control epidermal Langerhans cells were isolated from discarded skin, primarily elective circumcisions, from patients under 18 years of age. Control tonsil CD3 cells were isolated from discarded samples from elective tonsillectomy in patients under 18 years of age. Studies were performed according to protocols approved by the Institutional Review Board of Baylor College of Medicine.

Isolation of LCs and T Cells

LCH Samples—Fifteen fresh LCH biopsy samples were collected. They were transported in RPMI media (Invitrogen, Carlsbad, CA) and processed within 24 hours. All samples were processed into single cell suspension over a 70 uM mesh filter. Cells were washed twice with RPMI supplemented with 10% fetal bovine serum (FBS), then incubated with

conjugated antibodies, CD207-PE (Beckman Coulter, Fullerton, CA) and CD3-FITC (BD Bioscience, San Jose, CA) for 30 minutes on ice. Cells were washed again and resuspended in RPMI/FBS with 2 ug/ml propidium iodide (Molecular Probes, Eugene, OR). Cells were then separated by flow cytometry by gating on the propidium iodide-negative population and antibody-specific fluorescence. Cells were sorted with a MoFlo Sorter (Fullerton, CA) directly into PicoPure RNA Extraction Buffer (Molecular Devices, Sunnyvale, CA) (Supplemental Table IB). Select samples were re-analyzed by flow cytometry for purity (Figure 1).

Control Skin LC Samples—Control LCs were isolated from 12 skin samples that were transported in RPMI media, and processed within 24 hours. Tissue was incubated in RPMI with 5 units/ml dispase II (Roche, Indianapolis, IN) at 4°C for 8 hours prior to separation of the epidermal layer. The epidermal layer was further treated with 0.25% trypsin-EDTA (Invitrogen, Carlsbad, CA) for 15 minutes at 37°C, then Langerhans cells were isolated with CD207-PE conjugated antibody (Beckman Coulter, Fullerton, CA) as described above. Patient details from the individual skin samples were not available. However, review of elective circumcisions performed at Texas Children's Hospital in an operating room shows a range of ages from 1 month to 18 years.

Peripheral T Cells—Peripheral T cells were isolated from 7 patients with active LCH prior to chemotherapy (Supplemental Table I). Peripheral blood was collected and stored in EDTA+ tubes, then processed within 24 hours. Peripheral blood mononuclear cells were isolated after centrifuging blood over a Histopaque-1077 (Sigma-Aldrich, St. Louis, MO) gradient at 450G for 30 minutes. PBMCs were washed twice in RPMI, and then T cells were isolated with CD3-FITC (BD Bioscience, San Jose, CA) conjugated antibodies as described above.

Tonsil T Cells—T cells were isolated from 20 tonsil samples from children who underwent elective tonsillectomy. Tonsils were processed in an identical fashion to the LCH lesions, and CD3+ cells were isolated by flow cytometry with CD3-FITC antibody as described above.

RNA Purification and cDNA Amplification

Total RNA was processed and cDNA amplified for 13 LCH-CD207 samples, 12 control-CD207 samples, 12 LCH lesion-CD3 samples, 7 LCH-peripheral CD3 samples and 4 pooled tonsil-CD3 samples (5 individual RNA samples/tonsil pool). Total RNA was processed from the sorted cells according to the PicoPure RNA Isolation Kit protocol (Molecular Devices, Sunnyvale, CA). RNA concentration and quality was verified using the 6000 Pico Chip (Agilent, Santa Clara, CA) at the Baylor College of Medicine Microarray Facility. Any samples with a detectable RNA integrity number (14) (RIN)<5 were excluded from the study. cDNA amplification was performed with the WT-Ovation Pico System according to manufacturer's protocol (NuGen, San Carlos, CA). This is a whole-transcriptome amplification system with which we were able to generate 4–6 μg of cDNA from 700 pg-25 ng of input RNA. Fragmented and biotinylated cDNA samples for the gene chip studies were generated using the FL-Ovation cDNA Biotin Module v2 (Nugen, San Carlos, CA).

Affymetrix GeneChip Assays

Fragmented and biotinylated cDNA was hybridized to Affymetrix U133 Plus 2.0 chips (Affymetrix, Santa Clara, CA). cDNA was generated from each of the LCH-CD207, control-CD207, LCH lesion-CD3, and peripheral-CD3 samples and was used to hybridize onto individual chips. Four tonsil-CD3 cDNA were generated, each from 5 pooled cDNA samples. Chips were hybridized overnight at 45°C with 60 revolutions per min for 16 hours.

The chips were processed in the fluidic station using the FS450_004 wash and stain protocol according to manufacturer's instruction. The stained chips were scanned using the Affymetrix GeneChip scanner 3000. The datafiles have been deposited in the Gene Expression Omnibus website (http://www.ncbi.nlm.nih.gov/geo/; Accession number: GSE16395).

Data Analysis

Quality control of 48 Affymetrix U133 plus 2 gene expression chips was done using the BioConductor package affyQCReport (15). Beta actin and GAPDH ratios as well as signal distribution were assessed to determine the outlier cases. Normalization and probe set summarization was done in BRB-Arraytools (available at http://linus.nci.nih.gov/BRB-ArrayTools.html) using the Robust Multichip Average algorithm. Hierarchical clustering was performed using centered correlation and average linkage. The Significance Analysis of Microarrays algorithm (16) was used for analysis of differential expression with a False Discovery Rate (FDR) of less than 0.01. Samples were split into three groups for analysis. Group 1 consisted of 13 CD207 tumor samples and 12 CD207 controls obtained from normal skin. Group 2 consisted of 7 CD3 LCH lesion samples and 7 CD3 matched paired samples obtained from patients' peripheral blood. Group 3 consisted of 12 CD3 LCH lesion samples and 4 CD3 pooled controls obtained from tonsil. Heatmaps and other graphics were created using MultiExperiment Viewer, part of the TM4 Microarray Software Suite (17).

Quantitative Real Time PCR

Real-time PCR reactions were performed with TaqMan Gene Expression Assays (Applied Biosystems, Carlsbad, CA), which includes a mix of 2 unlabeled PCR primers (900 nM final concentration) and 1 FAM dye-labeled TaqMan MGB probe (250 nM final concentration). Single-stranded cDNA was generated by RNA amplification as described above in experiments independent from the amplifications used to generate cDNA probe for microarray studies. For the CD207+ analysis, one cDNA pool was made from equal contribution from the 13 LCH CD207+ samples and another from equal contribution from the 12 control CD207+ samples. For the CD3+ analysis, one cDNA pool was made from equal contribution from the 7 peripheral LCH CD3+ samples and another from equal contribution from the 7 matched LCH lesion CD3+ samples. Each reaction included 20 ng cDNA. TaqMan Fast Universal PCR Master Mix (Applied Biosystems) was used in 25 μl reactions in 96 well plates on a iQ5 Real Time PCR Detection System (Bio-Rad, Hercules, CA). Assays were plated in triplicate in two independent experiments. Thermal cycling conditions were set at 2 minutes at 50°C and 10 minutes at 95°C, then 40 cycles of 95°C and 60°C for 1 minute. Relative mRNA levels were determined using standard ddCt calculations, with expression levels of experimental samples normalized to GAPDH (18). Taqman probesets (Applied Biosytems) included AFF3, Hs00289335_s1; CCL5, Hs00174575_m1; CCR1, Hs00174298_m1; CD36, Hs01567188_g1; CD74, Hs00269961_m1; CDH1, Hs00170423_m1; CEACAM6, Hs00366002_m1; CTLA4, Hs00175480_m1; DCAL1, Hs00416849_m1; DUSP4, Hs01027785_m1; FOXP3, Hs00203958_m1; GAPDH, Hs02758991_g1; HLA-DRA, Hs00219578_m1; HOXB7, Hs00270131_m1; HSPA1A, Hs00359147_s1; IL17A, Hs00174383_m1; IL2, Hs00174114_m1; IL8, Hs00174103_m1; MMP1, Hs00899660_g1; MMP9, Hs00234579_m1; NRP1, Hs00826128_m1; PERP, Hs00751717_s1; S100A7, Hs00162488_m1; S100A8, Hs00374263_m1; SMYD3, Hs00224208_m1; SPP1, Hs00959010_m1; TACSTD1, Hs00158980_m1; TNFRSF9, Hs00155512_m1; and VNN1, Hs01546812_m1.

Immunohistochemistry

Fresh LCH biopsy tissue, skin samples and tonsil samples were snap frozen in embedding medium (Tissue-Tek O.C.T. Compound; Sakura Finetech USA Inc, Torrance, CA) for frozen tissue specimens and stored at −80°C within 8 hours from the time of collection. Tissue was cut at a thickness of 4–8μm from frozen blocks and adhered to microscope slides. Slides were stored at −80°C until use. After removal from storage, slides were air-dried for one half-hour and tissue was subsequently fixed by incubating slides in ice-cold acetone for 15 minutes. After being air-dried for 10 minutes, the tissue was then rehydrated by incubation in phosphate-buffered saline (PBS) for 10 minutes.

Immunohistochemical staining was performed using the Dako EnVision + Dual Link Kit (Carpinteria, CA). Endogenous peroxidase was blocked using Dako Block Buffer for 10 minutes. Primary antibodies were diluted in Dako Antibody Diluent and tissue incubated at room temperature for 3 hours or at 4°C overnight. Antibodies against CD11b and CD11c were diluted 1:10. All other antibodies were diluted 1:50. Mouse and rabbit antibodies were detected using the previously diluted HRP-linked secondary antibody included in the kit. Goat antibodies were detected using anti-goat/horseradish peroxidase (HRP) antibody (Dako) diluted 1:100. Slides were washed 3 times for 5 minutes each in Dako Wash Buffer between incubations. HRP activity was detected using Dako Liquid DAB+ Substrate Chromagen System. Tissue was then stained with hematoxylin, coverslipped and stored at room temperature. Antibodies used: **CD207 –** mouse monoclonal – ab49730 (Abcam, Cambridge, MA); **CD3 –** mouse monoclonal **–** ab699 (Abcam); **HLA-DR+DP+DQ –** mouse monoclonal sc59251 – (Santa Cruz Biotechnology, Santa Cruz, CA); **CTLA4 –** goat polyclonal – sc1628 (Santa Cruz Biotechnology); **Osteopontin –** mouse monoclonal – sc21742 (Santa Cruz Biotechnology); **CD44 –** rabbit monoclonal ab51037 – (Abcam); **Neuropilin1 –** mouse monoclonal – sc5307 (Santa Cruz Biotechnology); **Vanin1 –** goat polyclonal – sc16776 (Santa Cruz Biotechnology); **CEACAM6 –** rabbit polyclonal – ab56234 (Abcam); **MMP1 –** rabbit monoclonal – ab52631 (Abcam); **MMP9 –** goat polyclonal – sc6840 (Santa Cruz Biotechnology); **CD13 –** goat polyclonal –sc6995 (Santa Cruz Biotechnology); **CD33** rabbit polyclonal – ab59940 (Abcam); **CD1d –** mouse monoclonal – ab11076 (Abcam); **ICAM1 –** mouse monoclonal – ab20 (Abcam); **CD11b –** mouse monoclonal–MAB1699 (R&D Systems, Minneapolis, MN); **CD11c –** mouse monoclonal – MAB1777 (R&D Systems). Images were magnified using the Olympus BX51 microscope, 40X objective. Images were captured using the Olympus DP71 digital camera with Olympus DP Controller and DP Manager software.

Results

Robustness of the Gene Expression Profiling Procedures

Validity of the data derived from these gene expression profiling experiments is predicated on fidelity of the methods used to isolate cells and generate cDNA probe. Cells were sorted using fluorescent markers conjugated to CD3 and CD207 antibodies using standard methods (Figure 1). Cell purity was evaluated in several samples by sorting cells into RPMI, then re-analyzing with the MoFlo Sorter. Purity exceeded 95% in all CD3+ and CD207+ samples tested (Figure 1). The Nugen WT-Ovation Pico System was used to amplify RNA to generate cDNA probe for the gene expression profiling studies. The yield of cDNA consistently ranged between 4 μg and 6 μg. Previous studies have validated this experimental strategy (19,20). In this series of experiments, gene expression datasets generated from technical replicates of amplified probe from 5 ng input RNA had a correlation > 90% (data not shown).

Cell-specific gene expression from LCH biopsy specimens was evaluated by comparing hybridization signal from amplified cDNA on Affymetrix gene chips (U133A Plus 2.0) (Table I). Three sets of comparisons were performed: 1) Thirteen LCH CD207+ samples were compared to 12 control skin LCH CD207+ samples. 2) Seven LCH lesion CD3+ samples were compared to 7 peripheral blood CD3+ samples from the same patients. 3) Twelve LCH lesion CD3+ samples were compared to 4 pooled control tonsil CD3+ samples (5 individual tonsil CD3+ samples/pool). Validity of the data derived from this experimental strategy is evidenced by cell-specific grouping of the datasets in dendrograms constructed with unsupervised clustering (Supplemental Figure 1).

Cell-Specific Gene Expression Array Analyses

CD207+—Analysis of global gene expression in LCH-CD207 cells shows a consistent and distinct profile from control skin-CD207 cells, with overall correlation < 0.2. While the LCH-CD207 datasets are grouped with unsupervised clustering, the overall inter-group correlation > 30%. By comparison, the control skin-CD207 cells show less overall variability with an inter-group correlation > 50% (Supplemental Figure 1) (excluding Sample #1, which appears to be an outlier).

Expression of 2113 genes (out of >47,000) was significantly different between the LCH-CD207 cells and the control-CD207 cells using stringent statistical criteria (FDR<0.01). Overall, 747 probes (520 genes) showed increased expression and 2153 probes (1593 genes) showed decreased expression in the LCH-CD207 cells (Supplemental Data 1). Several genes involved in cell cycle regulation, inflammation and Langerhans cell development have been evaluated in LCH lesions and implicated in models of LCH pathogenesis. The most widely accepted current model of LCH can be described as the “Activated-Immature” model in which immature epidermal CD207+ Langerhans cells undergo malignant transformation, or pathologic immune stimulation, and subsequently take on some properties of an activated LC including down-regulation of anchoring molecules (*E-cadherin*) and increased expression of pro-inflammatory cytokines (*TNF-α IL-1β*), chemokine receptors (*CCR6, CCR7*), T cell co-stimulatory molecules (*CD40, CD80, CD86*), and markers of cell proliferation (*Ki67, PCNA*) (Reviewed in 8,10,21). Furthermore, several studies have described the LCH lesion microenvironment as a “cytokine storm”, with expression of several pro-inflammatory cytokines (10,21–24).

A comprehensive review of PubMed for genes and proteins associated with LCH pathogenesis was performed, and results were compared to cell-specific gene expression in this study (Figure 2, Supplemental Table IIA). Results from our study supported some previous observations, including significantly decreased expression of *E-cadherin* and relatively increased expression of *MMP9* (25,26 22,27,28). However, the lack of differential gene expression in many molecules previously associated with LCH was surprising. In some cases, such as *TNF-α* and *IL1-β*, genes were expressed at very highlevels in both control skin CD207+ cells and LCH lesion CD207+ cells. For others, such as *IL-2* and *IL-17A*, we failed to find significant levels of expression in either control epidermal or LCH lesion CD207+ cells. Additionally, some genes, such as *CCL20*, were not found to be significant despite high levels of expression in some LCH CD207+ samples due to highly variable expression. Specific results of differential expression of genes reportedly associated with LCH in these experiments are detailed below.

Further review of this dataset identified several genes of interest not previously associated with increased expression in LCH including genes involved in regulation of cell cycle (*CDC2A*, *AF4/FMR2 (member 3)*, *SMYD3*, *HOXB7*), apoptosis (*BAX*, *BCL2L1*, *CFLAR*) signal transduction (*DUSP4*, *JAK3*, *PRKCA*, *TLR2*, *TLR4*, *SOCS3*, *JAG2*), tumor invasion and metastasis/tissue invasion (*CEACAM6*, *MMP1*, *TGFβ1*), myeloid cell maturation

(*CD1D*, *CD13*, *CD14*, *CD33*, *ITGA2B*, *ITGAX*, *ITGAM*, *CD300F*) and lymphocyte trafficking (*SPP1*, *VNN1*, *NRP1*, *CCR1*). A large number of the genes with decreased or absent expression in the LCH-CD207 cells are involved in cell-cell adhesion, including *TACSTD1* (29). *PERP*, an apoptosis effector, is one of the genes with most significantly decreased expression in LCH-CD207 cells (30,31). *TIMP2*, a metalloproteinase inhibitor, also has reduced expression in LCH-CD207 cells (Figure 2, Supplemental Table IIA).

CD3+—Analysis of global gene expression in the LCH lesion-CD3 cells also shows a consistent and distinct profile from both the peripheral-LCH-CD3 cells and the tonsil control CD3 cells. Therefore, while lymphocytes from peripheral blood may factor into the variability of the gene expression profiles, these results suggest the CD3+ cells isolated from the LCH lesions primarily represent tumor infiltrating lymphocytes. Differential T cell populations within the LCH lesions may also contribute to the variability between the LCH lesion-CD3 datasets (Correlation >20%) compared to the peripheral LCH-CD3 datasets (Correlation>70%) or the control tonsil CD3 datasets (Correlation>70%) (Supplemental Figure 1).

Using stringent statistical criteria, 162 probe sets (129 genes) showed significant differences in hybridization between cDNA derived from CD3 cells isolated from LCH lesions and peripheral CD3 cells isolated from peripheral blood from the same at the time of biopsy. Overall, 117 probe sets (84 genes) had increased expression and 45 probe sets (45 genes) showed decreased expression in LCH lesion-CD3 cells (Supplemental Data 2). Differentially expressed genes in this group identify several markers of T cell activation including MHC Class II genes, *CD58*, *CD74* and *HSP70*. Interestingly, *FOXP3*, a gene specific to regulatory T cells (Tregs), was over-expressed in the LCH lesion-CD3 cells, supporting a similar observation reported by others (32). *CTLA4*, an activation marker associated with Tregs and inhibition of inflammation, was also overexpressed. LCH lesion infiltrating T cells also significantly overexpressed several genes involved in leukocyte chemotaxis including *SPP1*, *IL-8*, *CCL3*, *CCL16*, *CCR1*, *CCR5*, *Vitamin D Receptor* and *plasminogen activator/urokinase receptor*. *SPP1* had the highest relative expression in both the Group 1 (LCH-CD207 vs skin-CD207) and Group 2 (LCH lesion-CD3 vs LCH peripheral blood-CD3) datasets. *Dual specificity phosphatase 4* (*DUSP4*), a negative regulator of MAP kinase, was also highly over-expressed by both CD207 cells and CD3 cells from the LCH lesions (33) (Figure 3A, Supplemental Table IIB).

Comparing the 12 LCH lesion-CD3 samples and the 4 control tonsil-CD3 pooled samples, only 81 probe sets (70 genes) were significantly differentially expressed, all of which had decreased relative expression (Supplemental Data 3). Genes associated with an activated T_H1 (or T_H17) response, including *IL17*, *IL21*, and *CD40L*, were significantly under-expressed in LCH lesion T cells compared to control tonsil T cells (Figure 3B).

Validation

We performed real-time PCR (RT-PCR) on independently amplified cDNA samples to validate the microarray data. While there were some differences in amplitude of differences in relative gene expression determined by chip hybridization and RT-PCR in the Group 1 (LCH lesion CD207+ cells vs control CD207+ samples) and the Group 2 (LCH lesion CD3+ cells vs LCH peripheral CD3+ cells) samples, the trends were consistent. Quantitative differences with the two methodologies were likely due to signal compression with the chips at very high and baseline fluctuation of noise at very low levels of expression (Tables IA–IB).

Immunohistochemistry on a sample of LCH-associated proteins also substantiated the gene expression profiling data identified by the array experiments. Immunohistochemistry was

performed on four LCH biopsy samples as well as normal skin and tonsil biopsy samples used as controls for antibody staining. The results shown were reproducible and are representative of all LCH biopsy samples tested. Protein products of all of the candidate genes identified by these experiments as overexpressed in LCH lesions (CD207+ or CD3+ cells) were validated by immunohistochemistry (Figure 4).

Discussion

The concept that LCH arises from epidermal LCs was first proposed by the landmark observation by Nezelof that the histiocytes in LCH lesions contain Birbeck granules (11). Subsequently, cell-surface expression of langerin (CD207), a protein associated with Birbeck granules in antigen processing in LCs, was identified as pathognomonic of both normal LCs and pathological LCs in LCH. (34,35) Therefore models of LCH have developed around the concept of aberrant activation or malignant transformation of the resident epidermal Langerhans cell, as described above in the “Activated Immature Model” (Figure 5) (Reviewed in 8,10,21). However, results from our cell-specific gene expression analysis prompt us to question the origin of the LCH CD207+ cell. First, global expression patterns between control epidermal LCs and LCH CD207+ cells showed low overall correlation (Supplemental Figure 1). Furthermore, expression levels of specific genes central to the Activated Immature Model were not significantly different between the two groups in our experiments.

This study is the first to establish the gene expression profile of CD207+ cells isolated from patient LCH lesions, rather than from *in vitro* models derived from monocytes or monocyte-derived DCs. LCH-associated genes and proteins were identified through a comprehensive literature review, and relative LCH lesion CD207+ and CD3+ expression in this study are detailed in Figures 2–3 and Supplemental Table II. Differences between gene expression results from this study and some previously published observations may be due to the experimental limitations of immunohistochemistry including heterogeneity of LCH lesions, variable specificity of antibodies, and lack of reliable control tissues. It is also possible that tissue processing altered gene expression relative to cells that are fixed or frozen in tissue blocks.

This study was designed to identify gene expression patterns common to all LCH lesions. Datasets from all LCH CD207+ samples clustered in a group distinct from control epidermal LCs and with no distinction between the profiles from High Risk and Low Risk samples. Additional samples will be required to power a study to determine if there are significant cell-specific differences in gene transcription in biopsies from different patient groups.

In addition to testing previous concepts of LCH and associated markers, the experimental approach of cell-specific gene expression revealed some previously unrecognized patterns of gene expression. LCH CD207+ cells had increased expression of early myeloid markers compared to control epidermal LCs. Epidermal LCs are derived from myeloid precursors that take residence in the skin in embryonic life, but may be replenished by peripheral monocytes in inflamed skin (Reviewed in 36) (Figure 5A). Therefore, it has been difficult to understand how LCs, which are normally restricted to the epidermis, could give rise to such a multi-focal disorder. We recently identified in mice, a population of interstitial CD207+ (langerin+) DCs in most tissues including the lung, liver and lymph nodes. In contrast to LCs that are confined to the epidermis and derive from skin resident hematopoietic precursors, interstitial CD207+ DCs are derived from blood-borne precursor cells and are present in most of the tissues affected by LCH (36,37). Therefore, *langerin* expression is inducible and not exclusive to epidermal Langerhans cells. These observations, together with the results of the LCH gene expression studies presented here, suggest that LCH may

not derive from abnormal LCs, rather from abnormal circulating DC precursors. The observation that plasma M-CSF levels and myeloid dendritic cell precursors ($lin^-HLA\text{-}DR^+CD11c^+$) are over-abundant in patients with active LCH also supports bone-marrow derived precursors rather than epidermal LCs as the source of pathologic CD207+ cells in LCH (38).

We propose a model for LCH pathogenesis in which bone marrow-derived myeloid dendritic cell precursors rather than epidermal LCs migrate to sites of LCH lesions and differentiate into CD207+ cells (Figure 5C). In the "Misguided Myeloid Dendritic Cell Precursor" model, blood-derived myeloid dendritic cells are recruited to sites of disease where they accumulate and recruit activated T cells. Together, these cells elaborate mediators of inflammation and tissue destruction. These experiments do not answer the ongoing question of whether LCH arises from intrinsic defects in a transformed clonal population of precursor cells, or whether it is caused by a functional response to a pathologic stimulus. Lack of differential expression of markers of proliferation supports a model in which CD207+ LCH cells arise from accumulation of pathologic cells, which is also supported by other recent studies (32).

The role of T cells in LCH is not well-understood. There is no evidence of a functional interaction between T cells and CD207+ cells *in vivo* in LCH (39). Results from this study show highly variable ratios of CD207:CD3 cells in LCH lesions (Supplemental Table IB). The CD3 cells are unlikely to arise primarily from contamination of lesions at the time of biopsy since they have unique gene expression profiles when compared to peripheral blood (Supplemental Figure 1). Several genes with significant gene expression in LCH CD207+ play roles in lymphocyte activation, recruitment, and dendritic cell interaction including osteopontin, neuropilin-1 and vanin-1. Osteopontin, expressed by *SPP1*, also known as early T lymphocyte activation 1 (ETA-1), had the highest differential expression in both the *LCH CD207+ vs control LC* and *infiltrating LCH CD3+ vs peripheral LCH CD3+* datasets. It is a secreted phospoprotein with putative functions including T cell activation, Treg differentiation, homing of macrophages and T cells, cell survival and tumor progression (Reviewed in 40). Osteopontin-deficient mice have deficient type 1 immunity to bacterial and viral infections and are unable to form granulomas. (41) Osteopontin overexpression has been found in a variety of cancers, including breast cancer, lung cancer, colorectal cancer, stomach cancer, ovarian cancer, and melanoma (42). One of the major osteopontin ligands, CD44, is also significantly over-expressed in LCH CD207 cells compared to control LCs. Neuropilin-1, expressed by *NRP1*, is a membrane-bound co-receptor to a tyrosine kinase receptor for both vascular endothelial growth factor and semaphorin molecules. NRP1 is involved in axonal guidance of nerves. In the immune system, it is important in establishing the T cell-dendritic cell synapse as well as migration and adhesion of thymocytes (43,44). Vanin-1, expressed by *VNN1*, is a glycosylphosphatidylinositol (GPI)-anchored molecule expressed by perivascular thymic stromal cells that is essential in migration of hematopoietic progenitor cells to the thymus (45). Mice deficient in vanin-1 are unable to form granulomas in response to *Coxiella burnetti* infection (46). Increased expression of *SPP1*, *NRP1*, and *VNN1* by LCH CD207+ cells suggest a potentially interesting role for these genes in CD207+ cell- mediated recruitment of T cells to LCH lesions.

Multiple searches for a common antigen in LCH failed to identify an infectious etiology (Reviewed in 4). A recent study found that Tregs were enriched in LCH lesions as well as in peripheral blood of patients with active LCH. The same study found polyclonal T cell receptors rearrangements in DNA isolated from frozen biopsy samples (32). Regulatory T cells are thought to develop as an antigen-specific response. Similarly, activation of T cells typically arises through antigen-dependent mechanisms *in vivo*. The expression profile of infiltrating CD3 cells compared to circulating CD3 cells in patients with LCH is consistent

with an activated phenotype, and also supports enrichment of Tregs. Therefore, the mechanisms by which T cells are activated remain to be determined. Another recent study suggested LCH arises through expression of *IL-17A* by pathologic Langerhans cells. In our study, *IL-17A* expression was not detectable in CD207 cells, as described previously (47). Furthermore, relative expression of *IL-17A* and *IL-21* was significantly decreased in LCH lesion T cells compared to control tonsil T cells, suggesting LCH is not characterized by a TH1/TH17 response.

Conclusions

Improved understanding of the biology is essential to improve treatment of individuals with LCH. However, research in LCH is challenged by rare tissue samples and lack of reliable in vitro or animal models. We are now able to generate cDNA probe for expression studies from as few as 1500 cells The results show surprisingly distinct gene expression profiles between CD207+ cells from LCH lesions and control epidermal LCs, which suggests the LCH CD207+ cells are either highly differentiated, or arise from a distinct cell population. The relative expression of immature myeloid markers from the LCH CD207+ cells further supports a model in which LCH arises from a bone marrow-derived dendritic cell precursor rather than from a transformed resident epithelial Langerhans cell. The results from this study further identify several new genes that have not previously been associated with LCH that may be important diagnostic markers or therapeutic targets. Genes that encode osteopontin-1, neuropilin-1, and vanin-1, all of which are involved in lymphocyte trafficking and lymphocyte-dendritic cell communication, are highly expressed in LCH CD207+ cells. In summary, we propose a new model in which LCH does not arise from epidermal Langerhans cells, but from misguided myeloid dendritic cell precursors. Future studies will determine the definitive reclassification of “Histiocytosis X”.

Supplementary Material

Refer to Web version on PubMed Central for supplementary material.

Acknowledgments

We would like to thank Dr. Cliona Rooney for her helpful suggestions throughout this project. We would like to acknowledge Christopher Threeton, Michael Cubbage and Tatiana Goltsova of the TXCCC Flow Facility for their excellent technical support. Finally, we would also like to thank our colleagues who helped with collection of the LCH biopsy samples, as well as patients and families for their generous participation in this study.

Reference List

1. Carstensen H, Ornvold K. Langerhans-cell histiocytosis (histiocytosis X) in children. Ugeskr Laeger. 1993; 155:1779–1783. [PubMed: 8317026]
2. Arico M, Girschikofsky M, Genereau T, Klersy C, McClain K, Grois N, Emile JF, Lukina E, De JE, Danesino C. Langerhans cell histiocytosis in adults. Report from the International Registry of the Histiocyte Society. Eur J Cancer. 2003; 39:2341–2348. [PubMed: 14556926]
3. Arceci RJ. The histiocytoses: the fall of the Tower of Babel. Eur J Cancer. 1999; 35:747–767. [PubMed: 10505036]
4. McClain KL, Natkunam Y, Swerdlow SH. Atypical cellular disorders. Hematology Am Soc Hematol Educ Program. 2004:283–296. [PubMed: 15561688]
5. Gadner H, Grois N, Potschger U, Minkov M, Arico M, Braier J, Broadbent V, Donadieu J, Henter JI, McCarter R, Ladisch S. Improved outcome in multisystem Langerhans cell histiocytosis is associated with therapy intensification. Blood. 2008; 111:2556–2562. [PubMed: 18089850]

6. Gadner H, Grois N, Arico M, Broadbent V, Ceci A, Jakobson A, Komp D, Michaelis J, Nicholson S, Potschger U, Pritchard J, Ladisch S. A randomized trial of treatment for multisystem Langerhans' cell histiocytosis. J Pediatr. 2001; 138:728–734. [PubMed: 11343051]
7. Allen CE, McClain KL. Langerhans cell histiocytosis: a review of past, current and future therapies. Drugs Today (Barc). 2007; 43:627–643. [PubMed: 17940639]
8. Egeler RM, Annels NE, Hogendoorn PC. Langerhans cell histiocytosis: a pathologic combination of oncogenesis and immune dysregulation. Pediatr Blood Cancer. 2004; 42:401–403. [PubMed: 15049009]
9. Fadeel B, Henter JI. Langerhans-cell histiocytosis: neoplasia or unbridled inflammation? Trends Immunol. 2003; 24:409–410. [PubMed: 12909451]
10. Laman JD, Leenen PJ, Annels NE, Hogendoorn PC, Egeler RM. Langerhans-cell histiocytosis 'insight into DC biology'. Trends Immunol. 2003; 24:190–196. [PubMed: 12697451]
11. Nezelof C, Basset F. An hypothesis Langerhans cell histiocytosis: the failure of the immune system to switch from an innate to an adaptive mode. Pediatr Blood Cancer. 2004; 42:398–400. [PubMed: 15049008]
12. Willman CL, McClain KL. An update on clonality, cytokines, and viral etiology in Langerhans cell histiocytosis. Hematol Oncol Clin North Am. 1998; 12:407–416. [PubMed: 9561909]
13. Favara BE, Steele A. Langerhans cell histiocytosis of lymph nodes: a morphological assessment of 43 biopsies. Pediatr Pathol Lab Med. 1997; 17:769–787. [PubMed: 9267889]
14. Schroeder A, Mueller O, Stocker S, Salowsky R, Leiber M, Gassmann M, Lightfoot S, Menzel W, Granzow M, Ragg T. The RIN: an RNA integrity number for assigning integrity values to RNA measurements. BMC Mol Biol. 2006; 7:3. [PubMed: 16448564]
15. Gentleman RC V, Carey J, Bates DM, Bolstad B, Dettling M, Dudoit S, Ellis B, Gautier L, Ge Y, Gentry J, Hornik K, Hothorn T, Huber W, Iacus S, Irizarry R, Leisch F, Li C, Maechler M, Rossini AJ, Sawitzki G, Smith C, Smyth G, Tierney L, Yang JY, Zhang J. Bioconductor: open software development for computational biology and bioinformatics. Genome Biol. 2004; 5:R80. [PubMed: 15461798]
16. Tusher VG, Tibshirani R, Chu G. Significance analysis of microarrays applied to the ionizing radiation response. Proc Natl Acad Sci U S A. 2001; 98:5116–5121. [PubMed: 11309499]
17. Saeed AI, Sharov V, White J, Li J, Liang W, Bhagabati N, Braisted J, Klapa M, Currier T, Thiagarajan M, Sturn A, Snuffin M, Rezantsev A, Popov D, Ryltsov A, Kostukovich E, Borisovsky I, Liu Z, Vinsavich A, Trush V, Quackenbush J. TM4: a free, open-source system for microarray data management and analysis. Biotechniques. 2003; 34:374–378. [PubMed: 12613259]
18. Livak KJ, Schmittgen TD. Analysis of relative gene expression data using real-time quantitative PCR and the 2(-Delta Delta C(T)) Method. Methods. 2001; 25:402–408. [PubMed: 11846609]
19. Pradervand S, Paillusson A, Thomas J, Weber J, Wirapati P, Hagenbuchle O, Harshman K. Affymetrix Whole-Transcript Human Gene 1.0 ST array is highly concordant with standard 3′ expression arrays. Biotechniques. 2008; 44:759–762. [PubMed: 18476829]
20. Singh R, Maganti RJ, Jabba SV, Wang M, Deng G, Heath JD, Kurn N, Wangemann P. Microarray-based comparison of three amplification methods for nanogram amounts of total RNA. Am J Physiol Cell Physiol. 2005; 288:C1179–C1189. [PubMed: 15613496]
21. Bechan GI, Egeler RM, Arceci RJ. Biology of Langerhans cells and Langerhans cell histiocytosis. Int Rev Cytol. 2006; 254:1–43. [PubMed: 17147996]
22. Coury F, Annels N, Rivollier A, Olsson S, Santoro A, Speziani C, Azocar O, Flacher M, Djebali S, Tebib J, Brytting M, Egeler RM, Rabourdin-Combe C, Henter JI, Arico M, Delprat C. Langerhans cell histiocytosis reveals a new IL-17A-dependent pathway of dendritic cell fusion. Nat Med. 2008; 14:81–87. [PubMed: 18157139]
23. de Graaf JH, Tamminga RY, Dam-Meiring A, Kamps WA, Timens W. The presence of cytokines in Langerhans' cell histiocytosis. J Pathol. 1996; 180:400–406. [PubMed: 9014861]
24. Egeler RM, Favara BE, van MM, Laman JD, Claassen E. Differential In situ cytokine profiles of Langerhans-like cells and T cells in Langerhans cell histiocytosis: abundant expression of cytokines relevant to disease and treatment. Blood. 1999; 94:4195–4201. [PubMed: 10590064]

25. de Graaf JH, Tamminga RY, Kamps WA, Timens W. Expression of cellular adhesion molecules in Langerhans cell histiocytosis and normal Langerhans cells. Am J Pathol. 1995; 147:1161–1171. [PubMed: 7573361]
26. Geissmann F, Emile JF, Andry P, Thomas C, Fraitag S, De PY, Brousse N. Lack of expression of E-cadherin is associated with dissemination of Langerhans' cell histiocytosis and poor outcome. J Pathol. 1997; 181:301–304. [PubMed: 9155716]
27. da Costa CE, Annels NE, Faaij CM, Forsyth RG, Hogendoorn PC, Egeler RM. Presence of osteoclast-like multinucleated giant cells in the bone and nonostotic lesions of Langerhans cell histiocytosis. J Exp Med. 2005; 201:687–693. [PubMed: 15753204]
28. Hayashi T, Rush WL, Travis WD, Liotta LA, Stetler-Stevenson WG, Ferrans VJ. Immunohistochemical study of matrix metalloproteinases and their tissue inhibitors in pulmonary Langerhans' cell granulomatosis. Arch Pathol Lab Med. 1997; 121:930–937. [PubMed: 9302924]
29. Trzpis M, McLaughlin PM, de Leij LM, Harmsen MC. Epithelial cell adhesion molecule: more than a carcinoma marker and adhesion molecule. Am J Pathol. 2007; 171:386–395. [PubMed: 17600130]
30. Hildebrandt T, Preiherr J, Tarbe N, Klostermann S, van Muijen GN, Weidle UH. Identification of THW, a putative new tumor suppressor gene. Anticancer Res. 2000; 20:2801–2809. [PubMed: 11062687]
31. Ihrie RA, Marques MR, Nguyen BT, Horner JS, Papazoglu C, Bronson RT, Mills AA, Attardi LD. Perp is a p63-regulated gene essential for epithelial integrity. Cell. 2005; 120:843–856. [PubMed: 15797384]
32. Senechal B, Elain G, Jeziorski E, Grondin V, de Patey-Mariaud SN, Jaubert F, Beldjord K, Lellouch A, Glorion C, Zerah M, Mary P, Barkaoui M, Emile JF, Boccon-Gibod L, Josset P, Debre M, Fischer A, Donadieu J, Geissmann F. Expansion of Regulatory T Cells in Patients with Langerhans Cell Histiocytosis. PLoS Med. 2007; 4:e253. [PubMed: 17696642]
33. Guan KL, Butch E. Isolation and characterization of a novel dual specific phosphatase, HVH2, which selectively dephosphorylates the mitogen-activated protein kinase. J Biol Chem. 1995; 270:7197–7203. [PubMed: 7535768]
34. Valladeau J, Ravel O, zutter-Dambuyant C, Moore K, Kleijmeer M, Liu Y, Duvert-Frances V, Vincent C, Schmitt D, Davoust J, Caux C, Lebecque S, Saeland S. Langerin, a novel C-type lectin specific to Langerhans cells, is an endocytic receptor that induces the formation of Birbeck granules. Immunity. 2000; 12:71–81. [PubMed: 10661407]
35. Valladeau J, Duvert-Frances V, Pin JJ, zutter-Dambuyant C, Vincent C, Massacrier C, Vincent J, Yoneda K, Banchereau J, Caux C, Davoust J, Saeland S. The monoclonal antibody DCGM4 recognizes Langerin, a protein specific of Langerhans cells, and is rapidly internalized from the cell surface. Eur J Immunol. 1999; 29:2695–2704. [PubMed: 10508244]
36. Merad M, Ginhoux F, Collin M. Origin, homeostasis and function of Langerhans cells and other langerin-expressing dendritic cells. Nat Rev Immunol. 2008; 8:935–947. [PubMed: 19029989]
37. Ginhoux F, Tacke F, Angeli V, Bogunovic M, Loubeau M, Dai XM, Stanley ER, Randolph GJ, Merad M. Langerhans cells arise from monocytes in vivo. Nat Immunol. 2006; 7:265–273. [PubMed: 16444257]
38. Rolland A, Guyon L, Gill M, Cai YH, Banchereau J, McClain K, Palucka AK. Increased blood myeloid dendritic cells and dendritic cell-poietins in Langerhans cell histiocytosis. J Immunol. 2005; 174:3067–3071. [PubMed: 15728521]
39. Geissmann F, Lepelletier Y, Fraitag S, Valladeau J, Bodemer C, Debre M, Leborgne M, Saeland S, Brousse N. Differentiation of Langerhans cells in Langerhans cell histiocytosis. Blood. 2001; 97:1241–1248. [PubMed: 11222366]
40. Wang KX, Denhardt DT. Osteopontin: role in immune regulation and stress responses. Cytokine Growth Factor Rev. 2008; 19:333–345. [PubMed: 18952487]
41. Ashkar S, Weber GF, Panoutsakopoulou V, Sanchirico ME, Jansson M, Zawaideh S, Rittling SR, Denhardt DT, Glimcher MJ, Cantor H. Eta-1 (osteopontin): an early component of type-1 (cell-mediated) immunity. Science. 2000; 287:860–864. [PubMed: 10657301]

42. Rodrigues LR, Teixeira JA, Schmitt FL, Paulsson M, Lindmark-Mansson H. The role of osteopontin in tumor progression and metastasis in breast cancer. Cancer Epidemiol Biomarkers Prev. 2007; 16:1087–1097. [PubMed: 17548669]
43. Lepelletier Y, Smaniotto S, Hadj-Slimane R, Villa-Verde DM, Nogueira AC, Dardenne M, Hermine O, Savino W. Control of human thymocyte migration by Neuropilin-1/Semaphorin-3A-mediated interactions. Proc Natl Acad Sci U S A. 2007; 104:5545–5550. [PubMed: 17369353]
44. Tordjman R, Lepelletier Y, Lemarchandel V, Cambot M, Gaulard P, Hermine O, Romeo PH. A neuronal receptor, neuropilin-1, is essential for the initiation of the primary immune response. Nat Immunol. 2002; 3:477–482. [PubMed: 11953749]
45. Aurrand-Lions M, Galland F, Bazin H, Zakharyev VM, Imhof BA, Naquet P. Vanin-1, a novel GPI-linked perivascular molecule involved in thymus homing. Immunity. 1996; 5:391–405. [PubMed: 8934567]
46. Meghari S, Berruyer C, Lepidi H, Galland F, Naquet P, Mege JL. Vanin-1 controls granuloma formation and macrophage polarization in Coxiella burnetii infection. Eur J Immunol. 2007; 37:24–32. [PubMed: 17163446]
47. Allen CE, McClain KL. Interleukin-17A is not expressed by CD207(+) cells in Langerhans cell histiocytosis lesions. Nat Med. 2009; 15:483–484. [PubMed: 19424201]
48. Amir G, Weintraub M. Association of cell cycle-related gene products and NF-kappaB with clinical parameters in Langerhans cell histiocytosis. Pediatr Blood Cancer. 2008; 50:304–307. [PubMed: 17455317]
49. Schouten B, Egeler RM, Leenen PJ, Taminiau AH, van den Broek LJ, Hogendoorn PC. Expression of cell cycle-related gene products in Langerhans cell histiocytosis. J Pediatr Hematol Oncol. 2002; 24:727–732. [PubMed: 12468913]
50. Bank MI, Gudbrand C, Rengtved P, Carstensen H, Fadeel B, Henter JI, Petersen BL. Immunohistochemical detection of the apoptosis-related proteins FADD, FLICE, and FLIP in Langerhans cell histiocytosis. J Pediatr Hematol Oncol. 2005; 27:301–306. [PubMed: 15956881]
51. Annels NE, da Costa CE, Prins FA, Willemze A, Hogendoorn PC, Egeler RM. Aberrant chemokine receptor expression and chemokine production by Langerhans cells underlies the pathogenesis of Langerhans cell histiocytosis. J Exp Med. 2003; 197:1385–1390. [PubMed: 12743170]
52. de Graaf JH, Tamminga RY, Kamps WA, Timens W. Langerhans' cell histiocytosis: expression of leukocyte cellular adhesion molecules suggests abnormal homing and differentiation. Am J Pathol. 1994; 144:466–472. [PubMed: 7510455]
53. Rust R, Kluiver J, Visser L, Harms G, Blokzijl T, Kamps W, Poppema S, van den BA. Gene expression analysis of dendritic/Langerhans cells and Langerhans cell histiocytosis. J Pathol. 2006; 209:474–483. [PubMed: 16718746]
54. Vulcano M, Albanesi C, Stoppacciaro A, Bagnati R, D'Amico G, Struyf S, Transidico P, Bonecchi R, Del PA, Allavena P, Ruco LP, Chiabrando C, Girolomoni G, Mantovani A, Sozzani S. Dendritic cells as a major source of macrophage-derived chemokine/CCL22 in vitro and in vivo. Eur J Immunol. 2001; 31:812–822. [PubMed: 11241286]
55. Fleming MD, Pinkus JL, Fournier MV, Alexander SW, Tam C, Loda M, Sallan SE, Nichols KE, Carpentieri DF, Pinkus GS, Rollins BJ. Coincident expression of the chemokine receptors CCR6 and CCR7 by pathologic Langerhans cells in Langerhans cell histiocytosis. Blood. 2003; 101:2473–2475. [PubMed: 12642342]
56. Emile JF, Fraitag S, Leborgne M, De PY, Brousse N. Langerhans' cell histiocytosis cells are activated Langerhans' cells. J Pathol. 1994; 174:71–76. [PubMed: 7965409]
57. Ornvold K, Ralfkiaer E, Carstensen H. Immunohistochemical study of the abnormal cells in Langerhans cell histiocytosis (histiocytosis x). Virchows Arch A Pathol Anat Histopathol. 1990; 416:403–410. [PubMed: 2107627]
58. Ruco LP, Remotti D, Monardo F, Uccini S, Cristiani ML, Modesti A, Baroni CD. Letterer-Siwe disease: immunohistochemical evidence for a proliferative disorder involving immature cells of Langerhans lineage. Virchows Arch A Pathol Anat Histopathol. 1988; 413:239–247. [PubMed: 3135661]

59. Hage C, Willman CL, Favara BE, Isaacson PG. Langerhans' cell histiocytosis (histiocytosis X): immunophenotype and growth fraction. Hum Pathol. 1993; 24:840–845. [PubMed: 7690735]
60. Santegoets SJ, Gibbs S, Kroeze K, van d, Scheper VRJ, Borrebaeck CA, de Gruijl TD, Lindstedt M. Transcriptional profiling of human skin-resident Langerhans cells and CD1a+ dermal dendritic cells: differential activation states suggest distinct functions. J Leukoc Biol. 2008; 84:143–151. [PubMed: 18436579]
61. Egeler RM, Favara BE, Laman JD, Claassen E. Abundant expression of CD40 and CD40-ligand (CD154) in paediatric Langerhans cell histiocytosis lesions. Eur J Cancer. 2000; 36:2105–2110. [PubMed: 11044648]
62. Misery L, Rougier N, Crestani B, Faure M, Claudy A, Schmitt D, Vincent C. Presence of circulating abnormal CD34+ progenitors in adult Langerhans cell histiocytosis. Clin Exp Immunol. 1999; 117:177–182. [PubMed: 10403933]
63. Soilleux EJ, Coleman N. Langerhans cells and the cells of Langerhans cell histiocytosis do not express DC-SIGN. Blood. 2001; 98:1987–1988. [PubMed: 11565538]
64. Simonitsch I, Kopp CW, Mosberger I, Volc-Platzer B, Radaszkiewicz T. Expression of the monoclonal antibody HECA-452 defined E-selectin ligands in Langerhans cell histiocytosis. Virchows Arch. 1996; 427:477–481. [PubMed: 8624576]
65. Abdelatif OM, Chandler FW, Pantazis CG, McGuire BS. Enhanced expression of c-myc and H-ras oncogenes in Letterer-Siwe disease. A sequential study using colorimetric in situ hybridization. Arch Pathol Lab Med. 1990; 114:1254–1260. [PubMed: 2252422]
66. Petersen BL, Rengtved P, Bank MI, Carstensen H. High expression of markers of apoptosis in Langerhans cell histiocytosis. Histopathology. 2003; 42:186–193. [PubMed: 12558751]
67. Jaffe R, DeVaughn D, Langhoff E. Fascin and the differential diagnosis of childhood histiocytic lesions. Pediatr Dev Pathol. 1998; 1:216–221. [PubMed: 10463281]
68. Pinkus GS, Lones MA, Matsumura F, Yamashiro S, Said JW, Pinkus JL. Langerhans cell histiocytosis immunohistochemical expression of fascin, a dendritic cell marker. Am J Clin Pathol. 2002; 118:335–343. [PubMed: 12219775]
69. Emile JF, Tartour E, Brugieres L, Donadieu J, Le DF, Charnoz I, Fischer A, Fridman WH, Brousse N. Detection of GM-CSF in the sera of children with Langerhans' cell histiocytosis. Pediatr Allergy Immunol. 1994; 5:162–163. [PubMed: 7951757]
70. Emile JF, Fraitag S, Andry P, Leborgne M, Lellouch-Tubiana A, Brousse N. Expression of GM-CSF receptor by Langerhans' cell histiocytosis cells. Virchows Arch. 1995; 427:125–129. [PubMed: 7582241]
71. Bechan GI, Meeker AK, De Marzo AM, Racke F, Jaffe R, Sugar E, Arceci RJ. Telomere length shortening in Langerhans cell histiocytosis. Br J Haematol. 2008; 140:420–428. [PubMed: 18162125]
72. da Costa CE, Egeler RM, Hoogeboom M, Szuhai K, Forsyth RG, Niesters M, de Krijger RR, Tazi A, Hogendoorn PC, Annels NE. Differences in telomerase expression by the CD1a+ cells in Langerhans cell histiocytosis reflect the diverse clinical presentation of the disease. J Pathol. 2007; 212:188–197. [PubMed: 17447723]
73. Rosso DA, Ripoli MF, Roy A, Diez RA, Zelazko ME, Braier JL. Serum levels of interleukin-1 receptor antagonist and tumor necrosis factor-alpha are elevated in children with Langerhans cell histiocytosis. J Pediatr Hematol Oncol. 2003; 25:480–483. [PubMed: 12794527]
74. Ishii R, Morimoto A, Ikushima S, Sugimoto T, Asami K, Bessho F, Kudo K, Tsunematu Y, Fujimoto J, Imashuku S. High serum values of soluble CD154, IL-2 receptor, RANKL and osteoprotegerin in Langerhans cell histiocytosis. Pediatr Blood Cancer. 2006; 47:194–199. [PubMed: 16358318]
75. Rosso DA, Roy A, Zelazko M, Braier JL. Prognostic value of soluble interleukin 2 receptor levels in Langerhans cell histiocytosis. Br J Haematol. 2002; 117:54–58. [PubMed: 11918533]
76. Bank MI, Rengtved P, Carstensen H, Petersen BL. p53 expression in biopsies from children with Langerhans cell histiocytosis. J Pediatr Hematol Oncol. 2002; 24:733–736. [PubMed: 12468914]
77. Weintraub M, Bhatia KG, Chandra RS, Magrath IT, Ladisch S. p53 expression in Langerhans cell histiocytosis. J Pediatr Hematol Oncol. 1998; 20:12–17. [PubMed: 9482407]

78. Nakajima T, Watanabe S, Sato Y, Shimosato Y, Motoi M, Lennert K. S-100 protein in Langerhans cells, interdigitating reticulum cells and histiocytosis X cells. Gann. 1982; 73:429–432. [PubMed: 6982186]

79. Wu WS, McClain KL. DNA polymorphisms and mutations of the tumor necrosis factor-alpha (TNF-alpha) promoter in Langerhans cell histiocytosis (LCH). J Interferon Cytokine Res. 1997; 17:631–635. [PubMed: 9355965]

80. McClain KL, Laud P, Wu WS, Pollack MS. Langerhans cell histiocytosis patients have HLA Cw7 and DR4 types associated with specific clinical presentations and no increased frequency in polymorphisms of the tumor necrosis factor alpha promoter. Med Pediatr Oncol. 2003; 41:502–507. [PubMed: 14595706]

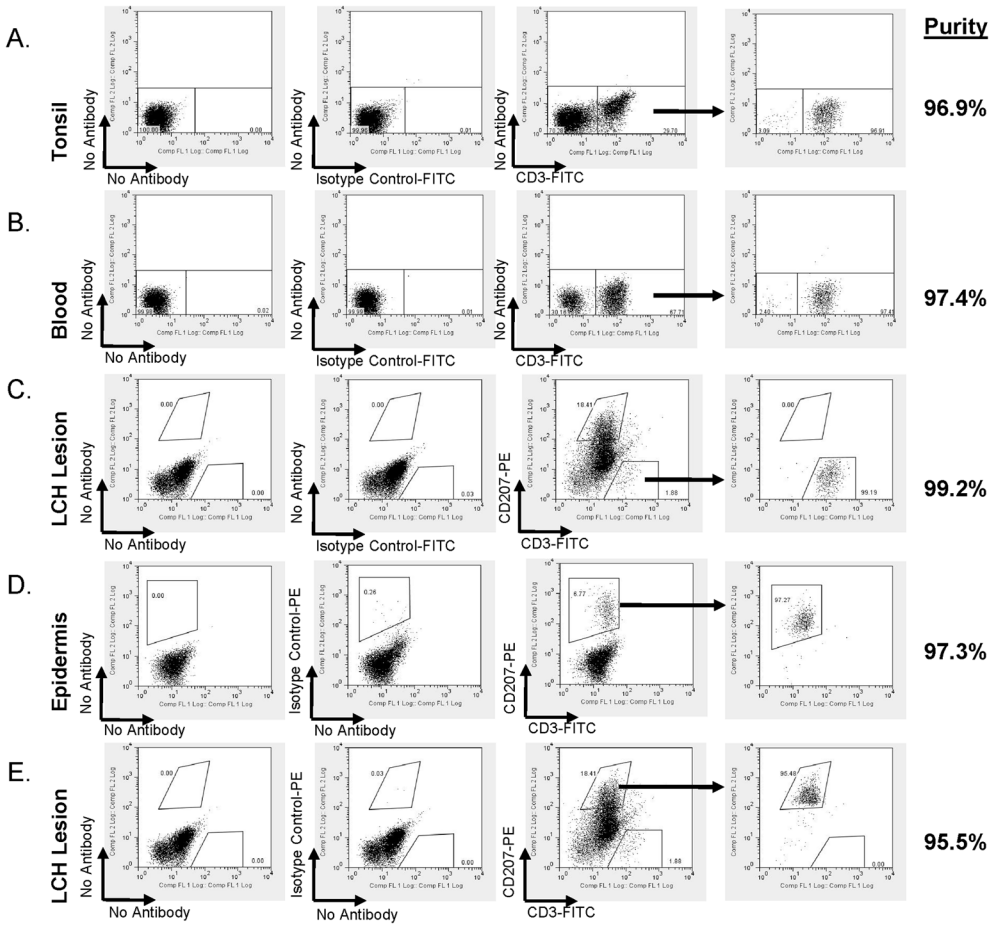

Figure 1. Scatter Plot of Cells Isolated Cells

Tissue samples were prepared as described in Methods. These images represents typical FACS studies from (A) control tonsil, (B) peripheral blood from LCH patients, (C)(E) LCH lesions, and (D) control skin (epidermis). The scanner was gated on PI-negative cells (living cells), and then CD207+ and CD3+ cells were purified with fluorescent conjugated antibodies. The scatter plots show results (right-to-left) with no antibody staining, isotype control, CD3+ and CD207+, then re-analysis of the sorted cells in a purity check. Sorted cell purity ranged from 95.5%–99.2% in these experiments. For the LCH lesions, CD3:CD207 ratio varies considerably from sample to sample (Supplemental Table IB), but the plot shown in (C) and (E) is a typical result and demonstrates the ability to obtain specific cell fractions from LCH lesions.

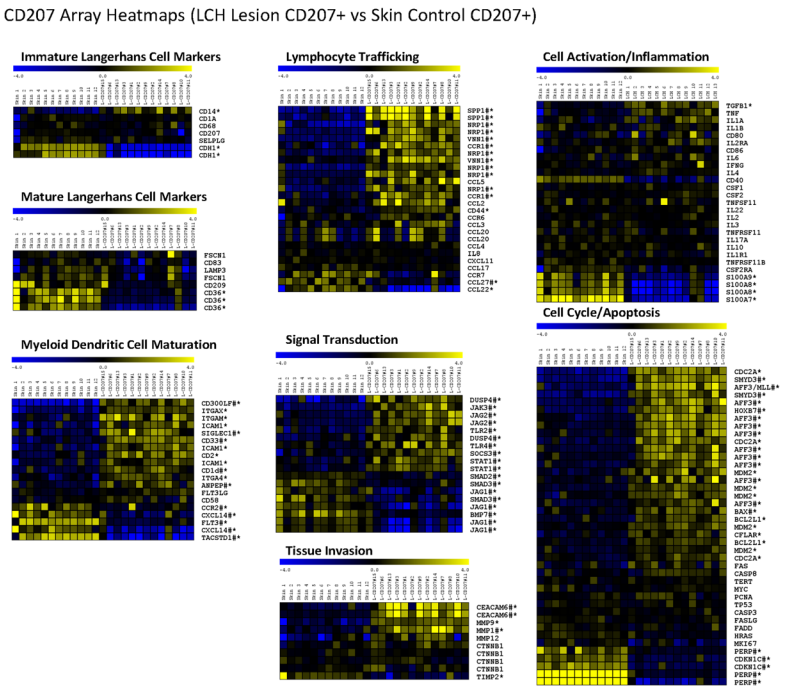

Figure 2. LCH-Associated Genes: CD207+

CD207+ (LCH Lesion CD207+ vs Skin CD207) Gene Heatmap

Literature was reviewed for genes associated with LCH, and tested for LCH CD207+-specific gene expression in our study. Genes with significant differential gene expression as determined by SAM analysis are identified in the heatmap with (*). Repeated sample names represent genes with multiple probes on the Affymetrix gene chip with significant results in the expression array experiments. Control skin sample CD207+ cells are listed on the left half of the figure. LCH CD207+ samples are listed on the right. Yellow boxes indicate increased expression in an individual sample. Blue indicates decreased expression. Some genes were not differentially expressed because expression was consistently high in both sets (example, *IL1B*). Some genes were not differentially expressed because expression was absent in both sets (example, *IL17A*). Some genes were not indicated as differentially expressed due to variability within the sets (example, *CCL20*). The categorical gene list indicates genes with significant increased (yellow) or decreased (blue) expression that may be relevant to LCH pathology and represent potential targets for diagnosis, prognosis and therapy. Several new genes not previously identified with LCH were identified (#), including genes involved in lymphocyte trafficking and myeloid dendritic cell-related integrins.

Genes/proteins previously associated with LCH

LCH CD207+ Array

BCL2L1 (48,49), CASP3 (48), CASP8 (50), CCL2 (10), CCL20/MIP-3α (51), CD44 (52), CCL22 (10,53,54), CCR6 (51), CCR7 (55), CD11b/ITGAM (25,52,56–58), CD11c/ITGAX (25,38,52,57), CD14 (39), CD1a (Reviewed in 3,4,10), CD2 (25,52,58,59), CD36 (60), CD40 (39,61), CD49d/ITGA4 (25), CD54/ICAM1 (25,52), CD58 (25,52), CD68 (57), CD80 (39), CD83 (39,62), CD86 (39), cdc2a/p16 (49), CD-SIGN/CD209 (63), CFLAR (50), CLA/SELPLG (64), c-myc (65), CXCL11/I-TAC (51), CXCL8/IL-8 (10), DC-LAMP/CD208 (39), E-cadherin/CDH1 (25,26), FADD (50), FAS (66), Fascin/FSCN1 (67,68), FASLG (66), FLT3LG (38), GMCSF/CSF2 (10,69,70), GM-CSFR/CSF2RA (70), H-ras (65), hTERT (71,72), IFNγ (10,23,24), IL-10 (10,32,39), IL-17A (22), IL1R1 (73), IL-1α (10,23,24), IL-1β (10,23,24), IL-2 (10,24), IL-22 (22), IL2Rα/CD25 (58,74,75), IL-3

(10,24), IL-4 (10,23,24), IL-6 (10), Ki67 (49,59), Langerin/CD207 (Reviewed in 3,4,10), M-CSF/CSF1 (38), MDM2 (49), MIP-1α/CCL3 (10), MIP-1β/CCL4 (10), MMP12 (22,53), MMP9 (22,27,28), Osteoprotegerin/TNFRSF11B (74,75), p53 (49,76,77), RANKL/TNFSF11 (22,23,74), RANK/TNFRSF11 (32), RANTES/CCL5 (51), S100A7 (78), S100A8 (78), S100A9 (78), TARC/CCL17 (10,53), TGF-β (10,23,24), TIMP2 (28), TNFα (10,24,25,79).

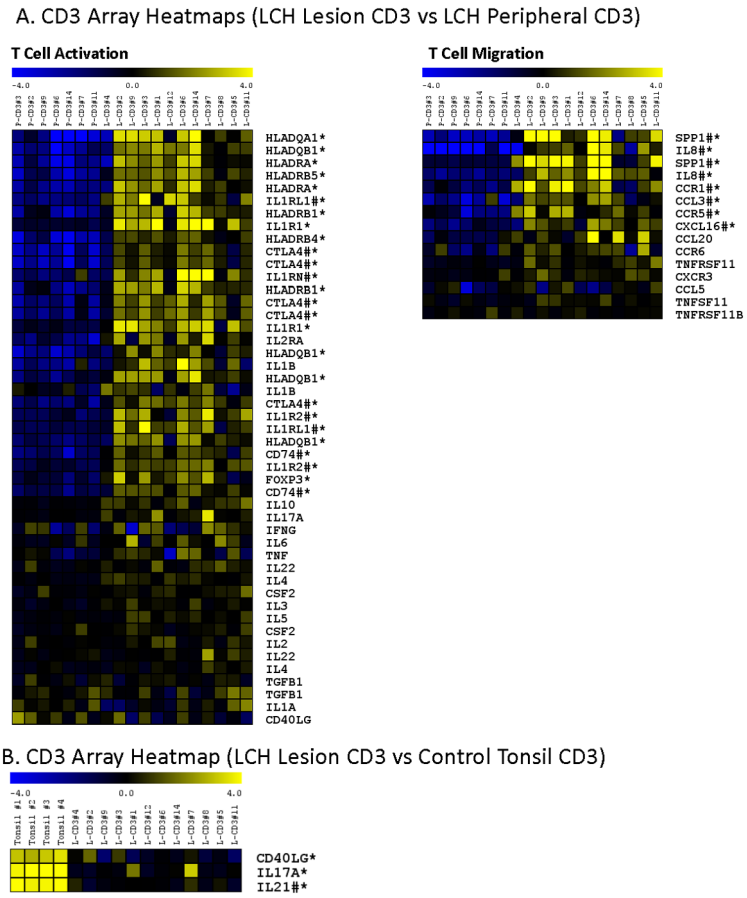

Figure 3. LCH-Associated Genes: CD3+

Figure 3A: LCH CD3+ (LCH Lesion CD3 vs LCH Peripheral CD3) Gene Heatmap

Expression profile results of CD3+ cells isolated from LCH lesions (LCH tumor CD3) (right) and CD3+ cells isolated from peripheral blood of patients with active LCH (LCH peripheral CD3) (left). The results from this comparison shows that genes associated with lymphocyte migration and activation have increased expression in tumor-infiltrating lymphocytes. This suggests that lymphocytes may play an active role in tumor formation and progression in LCH. Increased expression of *FOXP3* and *CTLA-4* specifically suggests over-representation of regulatory CD3+CD4+ T cells, which are thought to arise from antigen-driven activation. Osteopontin (SPP1) showed the highest relative expression in both LCH CD207+ cells and LCH lesion CD3+ cells.

Figure 3B: CD3+ (LCH Lesion CD3 vs Tonsil CD3) Gene Heatmap

Expression profile results of CD3+ cells isolated from LCH lesions (LCH tumor CD3) (right) and control CD3+ cells isolated from tonsils (left). These results suggest that, while LCH lesion T cells may be activated, they have significantly less expression of IL17 and IL21, associated with acute inflammation, compared to control tonsil T cells.

Genes/proteins previously associated with LCH

LCH CD3+ Arrays

CCL20/MIP3α (51), CCL5/RANTES (51), CCR6 (51), CD40LG (39,61,74), CXCR3 (10), FOXP3 (32), GMCSF/CSF2 (10,69,70), HLA-DR/DQ (10,39,80), IFN-γ (10,23,24), IL-10 (10,32,39), IL-17A (22), IL-1R1 (75), IL-1α (10,23,24), IL-1β (10,23,24), IL-2 (10,23,24), IL-22 (22), IL2Rα/CD25 (32,74), IL-3 (10,24), IL-4 (10,23,24), IL-5 (10,24), (IL-6) 10, TGF-β (10,23,24), TNFRSF11B (74,75), TNFSF11/RANKL (22,74), TNFα (10,24,25,79).

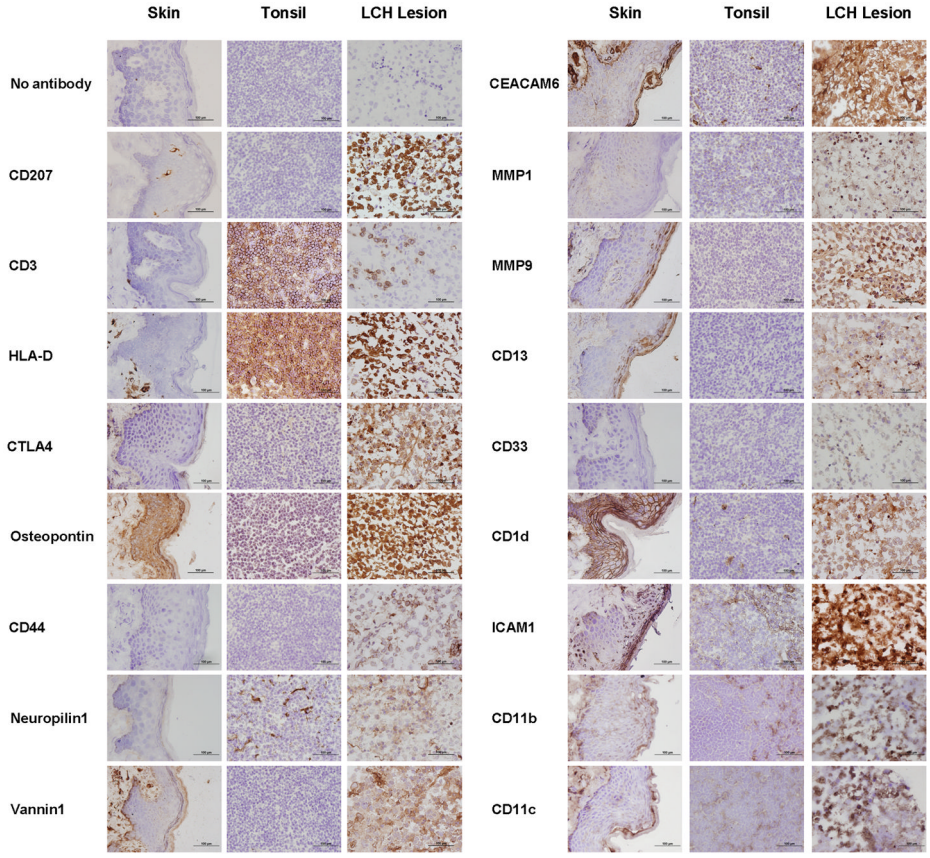

Figure 4. Immunohistochemistry of LCH-associated proteins

Immunohistochemistry with horseradish peroxidase-conjugated secondary antibodies was used to identify protein products of genes identified by the array experiments as overexpressed in LCH lesions. Normal skin and tonsil samples were used as controls for antibody staining. Images were magnified using the Olympus BX51 microscope, 40Xobjective. The black bar represents 100 μm. Immunohistochemistry images for each antibody are from a single LCH biopsy specimen, a single tonsil sample and a single skin sample and are representative of a series of 4 LCH lesions, 3 tonsil samples and 3 skin samples that were stained in the same manner.

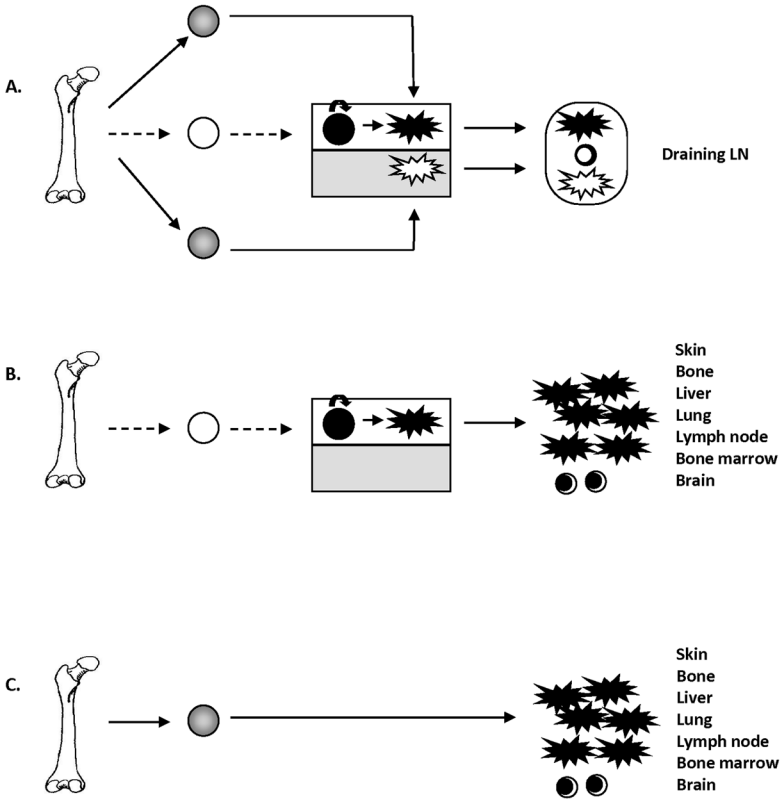

Figure 5. Models of Langerhans Cell Function and LCH

Figure 5A. Epidermal Langerhans Cells and Dermal CD207+ Dendritic Cells

Two CD207+ dendritic cell populations have been described: epidermal LCs and dermal dendritic cells 36. Langerhans cells (black star) are derived from self-renewing radio-resistant precursors (black circle) that migrate to epidermis (white box) during fetal life(white sphere, dashed arrow). In order to maintain homeostasis after injury or inflammation, monocytes (gray circle) may migrate to the epidermis where they differentiate into LCs. Epidermal LCs are thought to process antigen, then undergo activation via pro-inflammatory cytokines, down-regulate adhesion molecules, and migrate to draining lymph nodes where they present antigen to effector T cells (black/white circles). CD207+ dermal dendritic cells (white star) are a transitory cell population derived from myeloid dendritic cell precursors that migrate through the dermis (gray box) and, like LCs, present antigen to effector T cells.

Figure 5B. The Immature-Activated Model of LCH

LCH is currently thought to arise from pathologic epidermal LCs (black star) that either undergo malignant transformation or proliferate due to immune dysregulation and form lesions in skin, bone, liver, lung, lymph node, bone marrow or brain. T cells are present in LCH lesions (black/white circles), but do not have functional interactions with the pathologic LCs.

Figure 5C. The Misguided Myeloid Dendritic Cell Precursor Model

Based on results from our study, we hypothesize that LCH lesions may arise directly from bone marrow-derived myeloid dendritic cell precursors (gray circle). Pathologic dendritic cells acquire CD207 antigen expression as they home to sites of disease. The CD207+ LCH cells express factors that attract T cells to the lesions, with enrichment of a regulatory T cell population.

Table I

Comparison of Real-Time PCR (RT-PCR) and Microarray Results

Table IA. LCH CD207 vs. Control Skin CD207		
	RT-PCR	**Array**
SPP1	162.6	22.5–37.0
CEACAM6	76.7	10.1
CDK2NA	73.9	2.1–4.9
JAK3	46.1	1.9–7.1
VNN1	44.0	5.2–7.7
SMYD3	34.8	9.3–12.4
AFF3	24.7	3.1–11.3
HOXB7	20.7	6.6–6.8
DUSP4	15.7	3.4–10.3
MMP9	15.5	7.6
MMP1	11.5	7.2
CCR1	8.6	4.5–5.7
CCL5	8.6	4.6
NRP1	4.8	4.5–9.5
TNFRSF9	4.6	5.8–6.4
DCAL1	3.2	5.1–6.6
CD36	−28.1	− (1.4—14.4)
S100A8	−60.2	− (22.5—26.2)
EpCAM	−204.4	−38.1
CDH1	−269.6	− (32.2—123.6)
PERP	−1172.0	− (3.9—227.5)
S100A7	−14201.0	− (1.7—74)
IL-2	NA	1.0
IL-17	NA	1.1

Table IB. LCH Lesion CD3 vs. LCH Peripheral CD3		
	RT-PCR	**Array**
SPP1	50031.3	38.9–69.4
IL8	572.6	21.6–45.7
MMP9	219.9	43.6
HSPA	40.8	15.3–21.8
FOXP3	24.7	6.7
HLADR	18.9	11.6–22.0
CTLA4	11.4	7.5–13.4
DUSP4	10.3	6.7–54.6
CD74	5.7	5.2–6.2

Representative genes identified by CD207 gene expression array studies are listed in the left column. The fold-change (LCH LC vs. control skin LC) as determined by real-time PCR is listed in the middle column. The fold-change as determined by microarray is listed on the right. There are multiple values for some of the array data due to multiple probes for different regions of a single gene on the array chips which are represented by ranges. Changes are more pronounced in the RT-PCR assays, likely due to the lack of signal compression. In the chip studies, even if gene expression is absent, background signal may be interpreted as minimal expression. In general, RT-PCR confirms trends of increased and decreased expression in candidate genes identified by the gene chip studies. Similarly, RT-PCR fails to identify significant differences in some genes previously associated with LCH. “N/A” indicates that no PCR product was amplified in the RT-PCR reaction, suggesting absence of target template for *IL-2* and *IL-17*.

Data are organized as described above for array and real-time PCR experiments using cDNA generated from purified CD3 cells.